

## ARTICLE

## Application of a ferrocene-chelating heteroscorpionate ligand in nickel mediated radical polymerization

Received 00th January 20xx,  
Accepted 00th January 20xx

DOI: 10.1039/x0xx00000x

Shuangshuang Li,<sup>a,b</sup> Ashton R. Davis,<sup>c</sup> Hootan Roshandel,<sup>c</sup> Nima Adhami,<sup>c</sup> Yi Shen,<sup>c</sup> Nathalie H. Co,<sup>c</sup> Leo A. Morag,<sup>c</sup> Hafez Etemad,<sup>c</sup> Yuan Liu,<sup>b</sup> Paula L. Diaconescu<sup>\*c</sup>

A nickel bromide complex supported by a non-innocent ferrocene-chelating heteroscorpionate ligand,  $[(fc(PPh_2)(BH(3,5-Me_2pz)_2)NiBr)]$  ( $fc^{P,B}$ )NiBr, ( $fc$  = 1,1'-ferrocenediyl,  $pz$  = pyrazole), was synthesized and characterized. The compound can be readily oxidized according to UV-vis and  $^1H$  NMR spectroscopy. The catalytic activity of the compound's different oxidation states in the polymerization of vinyl monomers was explored. AB and ABA-type block copolymers were made from styrene and *p*-chlorostyrene, offering an example of orthogonal redox control in radical polymerization.

### Introduction

Redox switchable catalysis has been gaining traction over the past decade as a method to obtain control over polymer architecture by changing electron density at either the ligand framework or the metal center.<sup>1-7</sup> The use of external stimuli such as chemical redox agents or electricity to control the oxidation states of catalysts can be exploited to turn on and off different complementary catalytic reactions.<sup>8-11</sup> This form of orthogonal reactivity has been extensively explored by our group<sup>12-17</sup> and others<sup>18-25</sup> in ring open polymerization of cyclic esters and ethers, yet there has been a limited number of attempts to expand the scope of redox controlled systems.<sup>1,7,26-36</sup>

Nickel halide complexes, particularly nickel bromides,<sup>37-39</sup> in the presence of an initiator, are active radical polymerization systems with notable examples in atom transfer radical polymerization (ATRP, Figure 1a).<sup>40,41</sup> The rates of polymerization and equilibria in ATRP can be influenced via changes in the redox state of the supporting ligand in metal halide species.<sup>42</sup> While ferrocene systems in conjunction with copper have been previously investigated,<sup>43</sup> the influence of the redox states of ferrocene on monomer activity and selectivity has not been investigated. Therefore, we set out to probe the effects of redox states in radical polymerization with the goal of expanding the scope of active systems for redox switchable catalysis.

We previously reported ferrocene-chelating heteroscorpionate metal complexes in order to synthesize olefinic copolymers by utilizing a chemical redox switch.<sup>44</sup>

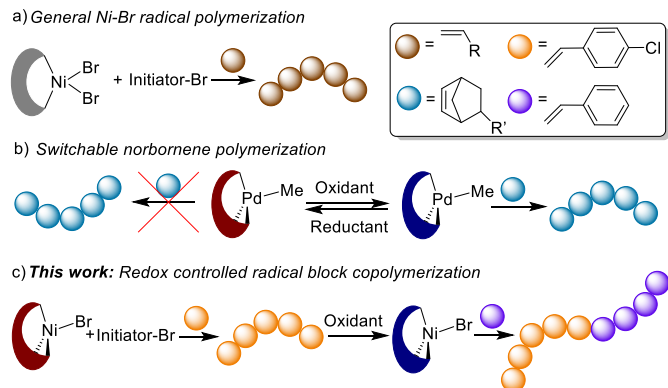


**Figure 1.** (a) General Ni-Br radical polymerization. (b) Switchable behavior of ( $fc^{P,B}$ )PdMe in norbornene polymerization.<sup>45</sup> (c) Redox dependent behavior of ( $fc^{P,B}$ )NiBr in radical block copolymerizations.

The palladium alkyl heteroscorpionate  $[(fc(PPh_2)(BH(3,5-Me_2pz)_2)PdMe)]$  ( $fc^{P,B}$ )PdMe, ( $fc$  = 1,1'-ferrocenediyl,  $pz$  = pyrazole) was successfully used as a catalyst in the switchable polymerization of norbornene derivatives; albeit only one oxidation state was catalytically active (Figure 1b).<sup>45</sup> A brief foray into nickel chemistry revealed an incompatibility in redox behaviors of the iron contained in the ferrocene moiety and nickel, unlike what was observed with the palladium system.<sup>44</sup> Particularly, in the case of the nickel alkyl complex ( $fc^{P,B}$ )NiMe, the tendency of both metals to undergo one electron redox processes at similar potentials results in an irreversible loss of the alkyl ligand, rendering this compound unfit for redox-switchable polymerization of vinyl monomers. However, the nickel halide complex, ( $fc^{P,B}$ )NiCl, displays two distinct redox events, which can be attributed to the supporting ligand and nickel. The reversibility of these events warrants further investigation into the nickel halide heteroscorpionate and their potential application in redox switchable catalysis. Since nickel bromide compounds used in

<sup>a</sup> Laboratory of Reaction and Separation Technology, College of Chemistry and Pharmaceutical Sciences, Qingdao Agricultural University, Qingdao 266109, China

<sup>b</sup> Department of Catalysis Science and Technology, School of Chemical Engineering, Tianjin University, Tianjin 300350, China

<sup>c</sup> Department of Chemistry and Biochemistry, University of California, Los Angeles 607 Charles E. Young Drive East Los Angeles CA 90095, USA

E-mail: pld@chem.ucla.edu

†Electronic Supplementary Information (ESI) available. CCDC 2279683. For ESI see DOI: 10.1039/x0xx00000x

radical polymerization have historically given better polymer properties than nickel chloride species,<sup>39,46-49</sup> we set out to investigate whether  $(fc^{P,B})NiBr$  would be a good candidate for radical polymerization of vinyl monomers utilizing the principles of redox switchable catalysis (Figure 1c).

Herein, we report the synthesis and characterization of a ferrocene-based heteroscorpionate nickel halide complex,  $(fc^{P,B})NiBr$ , which shows excellent orthogonal reactivity in two different oxidation states. A monomer screen, consisting of styrene, *p*-chlorostyrene (*p*-CS), methyl methacrylate (MMA), *n*-butyl methacrylate (*n*-BuMA), and acrylonitrile was conducted. As a proof-of-concept, AB and ABA type block copolymers of styrene and *p*-chlorostyrene were also synthesized by the sequential addition of monomers and redox reagents.

## Experimental Section

### General Considerations

All experiments were performed under a dry nitrogen atmosphere in an MBraun glovebox or using standard Schlenk techniques unless otherwise noted. Solvents were purified using a two-column solid-state purification system by the method of Grubbs<sup>50</sup> and transferred to the glovebox without exposure to air. NMR solvents were obtained from Cambridge Isotope Laboratories, degassed, and stored over activated molecular sieves prior to use. NMR spectra were recorded on Bruker AV-300, Bruker AV-400, Bruker DRX-500, or Bruker AV-600 spectrometers at room temperature unless otherwise noted. Chemical shifts are reported with respect to the residual solvent peaks, 7.16 ppm ( $C_6D_6$ ) and 7.26 ( $CDCl_3$ ) for  $^1H$  NMR spectra. The monomers and 1,2-difluorobenzene (DFB) were purchased from Sigma Aldrich or Fisher Scientific and distilled over  $CaH_2$  and then brought into the glovebox without exposure to air.  $(fc^{P,B})Li(THF)_2$ <sup>44,45</sup> and  $FcBAr^F$  ( $Fc$  = ferrocenium,  $BAr^F$  = tetrakis(3,5-bis(trifluoromethyl)-phenyl)borate)<sup>51</sup> were prepared according to literature procedures and, unless otherwise noted, all reagents were acquired from commercial sources and used as received. Elemental analysis of the reduced and the oxidized compound was performed using an Exeter Analytical, Inc. CE-440 elemental analyzer. The molecular weights of the polymers were determined using a SEC-MALS instrument at UCLA. SEC-MALS uses a Shimazu Prominence-i LC 2030C 3D equipped with an autosampler, two MZ Analysentechnik MZ-Gel SDplus LS 5  $\mu m$ , 300  $\times$  8 mm linear columns, a Wyatt DAWN HELEOS-II, and a Wyatt Optilab T-rEX. The column temperature was set at 40 °C. The flow rate of the column was kept at 0.70 mL min<sup>-1</sup> and samples were dissolved in THF. The number average molar mass and dispersity values were  $d_n/dc$  values, which were calculated by 100% mass recovery from the RI signal, attributed to the dominant feature in the trace.

### Synthesis of $(fc^{P,B})NiBr$

To  $NiBr_2(DME)$  ( $DME$  = 1,2-dimethoxyethane, 0.318 g, 1.03 mmol) in 7 mL THF, a solution of  $(fc^{P,B})Li(THF)_2$  (0.729 g, 0.938 mmol) in 2 mL THF was added dropwise at ambient temperature, and the color of the solution changed rapidly from orange to dark greenish-black. The reaction solution was stirred for 2 h. After removal of volatiles under reduced pressure, the product was extracted into 8 mL of toluene, and then filtered through Celite. Reduction in the volume of

toluene to about 7 mL under a reduced pressure and layering of 10 mL of hexanes afforded a dark green crystalline material after 24 hours at -35 °C. Decanting of the solution and washing of the remaining solids with 3 mL of cold hexanes yielded the product as a dark green crystalline material (0.52 g, 69.1%). X-ray quality crystals were obtained from a solution of toluene layered with hexanes at -40 °C. The compound is paramagnetic.  $^1H$  NMR (500 MHz, 25 °C,  $C_6D_6$ ):  $\delta$  (ppm) 19.50 (s, br), 14.62 (s, br), 12.02 (s, br), 4.53(s), 3.34 (s, br), -5.61 (s, br), -10.26 (s, br).  $^{13}C$  NMR (126 MHz, 25 °C,  $C_6D_6$ ):  $\delta$  (ppm) 125.70 (s, br, aromatic), 99.75 (s, br, CH), 79.44 (s, Cp-C), 70.89 (s, br, Cp-C), 67.38 (s, Cp-C), 24.32 (s, br, CCH<sub>3</sub>).  $^{31}P$  NMR (121 MHz, 25 °C,  $C_6D_6$ ):  $\delta$  (ppm) 10.26 (s). Anal.  $(fc^{P,B})NiBr \cdot (C_7H_8)$  ( $C_{39}H_{41}BBrFeN_4NiP$ ) calcd: C, 58.4; H, 5.11; N, 6.98. Found: C, 58.8; H, 5.13; N, 7.12.

### Isolation of $[(fc^{P,B})NiBr][BAr^F]$

A solution of  $FcBAr^F$  (70.1 mg, 0.067 mmol) in 1,2-difluorobenzene (DFB, 1 mL) was added to a stirring solution of  $(fc^{P,B})NiBr$  (53.6 mg, 0.067 mmol) in DFB (1 mL) and allowed to react for 2 h before removing the volatiles under a reduced pressure. The oily residual was washed with cold hexanes three times and benzene was added to redissolve the product. After letting it stand at -35 °C overnight, the solution was decanted, and the remaining dark brown oil was dried *in vacuo* for 12 h (90.1 mg, 81%). The compound readily decomposes if heated above room temperature, limiting the polymerization reactions to temperatures equal or less than 25 °C. Attempts to grow crystals of the oxidized compound were unsuccessful. There are no obvious peaks in the corresponding  $^1H$  NMR (500 MHz, 25 °C,  $C_6D_6$ ) spectrum. Anal.  $[(fc^{P,B})NiBr][BAr^F] \cdot (C_7H_8)$  ( $C_{71}H_{53}B_2BrFeN_4NiPF_{24}$ ) calcd: C, 51.2; H, 3.18; N, 3.36. Found: C, 51.5; H, 3.11; N, 3.41.

### Homopolymerizations with $(fc^{P,B})NiBr$

Under an inert atmosphere,  $(fc^{P,B})NiBr$  (11.1  $\mu$ mol) in 0.2 mL DFB, ethyl 2-bromo isobutyrate (11.1  $\mu$ mol) in 0.1 mL  $C_6D_6$ , 1,3,5-trimethoxybenzene (TMB, 0.117 mmol) in 0.1 mL  $C_6D_6$ , and monomer (1.05 mmol) were added to a J-Young NMR tube. The reaction mixture was shaken occasionally. The tube was sealed and brought out of the glovebox and placed in an oil bath when heating was required. The NMR tube was taken out of the oil bath and the monomer conversion was monitored by  $^1H$  NMR spectroscopy. When the desired conversion was reached,  $CH_2Cl_2$  was added to dissolve the polymer and the resulting solution was poured into 10 mL of cold methanol to precipitate the polymer; the mixture was centrifuged for 5 min, and the supernatant was decanted. This process was repeated twice to remove the catalyst and unreacted monomer. Polymers containing *p*-chlorostyrene were quenched with acetone and precipitated with ethanol acidified with hydrochloric acid (wt. 5 %) instead of  $CH_2Cl_2$  and methanol. The resulting polymer was dried under a reduced pressure before characterization.

### Homopolymerization with *in situ* generated $[(fc^{P,B})NiBr][BAr^F]$

Under an inert atmosphere,  $FcBAr^F$  (11.1  $\mu$ mol) in 0.1 mL DFB was added dropwise to a stirring solution of  $(fc^{P,B})NiBr$  (11.1  $\mu$ mol) in 0.2 mL DFB. After 2 h, the solution was filtered through Celite and added to a J-Young NMR tube with ethyl 2-bromo isobutyrate (11.1  $\mu$ mol) in 0.1 mL  $C_6D_6$ , TMB (0.1167 mmol) in 0.1 mL  $C_6D_6$ , monomer (1.05 mmol). The reaction mixture was left at room temperature while being shaken occasionally. If heated, the compound will degrade to

form an insoluble black powder. The tube was sealed and brought out of the glovebox and monomer conversion was monitored by  $^1\text{H}$  NMR spectroscopy.

#### General procedure for copolymerization

Under an inert atmosphere,  $(\text{fc}^{\text{P},\text{B}})\text{NiBr}$  (11.1  $\mu\text{mol}$ ) in 0.2 mL DFB and TMB (0.1167 mmol) in 0.1 mL  $\text{C}_6\text{D}_6$  were added to a J-Young NMR tube. If starting with the oxidized compound,  $\text{FcBAr}^{\text{F}}$  (11.1  $\mu\text{mol}$ ) in 0.1 mL DFB was added and allowed to react for 2 h followed by ethyl 2-bromoisoctyrate (11.1  $\mu\text{mol}$ ) in 0.1 mL  $\text{C}_6\text{D}_6$ . Otherwise, ethyl 2-bromoisoctyrate (11.1  $\mu\text{mol}$ ) in 0.1 mL  $\text{C}_6\text{D}_6$  was added immediately. The NMR tube was charged with monomer (1.05 mmol), sealed, brought out of the glovebox, and placed in an oil bath when a higher than ambient temperature was needed. Monomer conversion was measured by  $^1\text{H}$  NMR spectroscopy. When a desired conversion was reached, the NMR tube was brought back into the glovebox, and  $\text{CoCp}_2$  (11.1  $\mu\text{mol}$ ) or  $\text{FcBAr}^{\text{F}}$  (11.1  $\mu\text{mol}$ ) in 0.1 mL DFB was added at room temperature. The reaction mixture was left at room temperature for either 15 min or 2 h, respectively, with occasional shaking before the next monomer was added. This process was repeated for the synthesis of triblock copolymers. For polymerization reactions with styrene as the first and/or last monomer in the chain, we observed some auto-polymerized species that were co-isolated with the desired polymer species in small but noticeable amounts.

#### General procedure for polymer isolation

When the desired conversion was reached,  $\text{CH}_2\text{Cl}_2$  was added to dissolve the polymer and the resulting solution was poured into 10 mL of cold methanol to precipitate the polymer; the mixture was centrifuged for 5 minutes, and the supernatant was decanted. This process was repeated twice to remove the catalyst and unreacted monomer. Polymers containing *p*-chlorostyrene were quenched with acetone and precipitated with ethanol acidified with hydrochloric acid (5% wt.) instead of  $\text{CH}_2\text{Cl}_2$  and methanol. This method was not able to wash out some of the heavier oligomeric products from the bulk polymer samples. The resulting polymer was dried under reduced pressure before characterization.

#### Cyclic voltammetry study of $(\text{fc}^{\text{P},\text{B}})\text{NiBr}$

Cyclic voltammetry studies were conducted using a 20 mL scintillation vial with electrodes fixed in position by a rubber stopper, in a 0.10 mM tetrabutylammonium hexafluorophosphate ( $\text{TBAPF}_6$ ) solution in THF. A glassy carbon working electrode (planar circular area = 0.071  $\text{cm}^2$ ), a platinum reference electrode (planar circular area = 0.031  $\text{cm}^2$ ), and a silver-wire pseudoreference electrode (purchased from CH Instruments) were used. Before starting, the working and auxiliary electrodes were polished with an aqueous suspension of 1.00  $\mu\text{m}$ , 0.30  $\mu\text{m}$ , followed by 0.05  $\mu\text{m}$  alumina on a Microcloth polishing pad with a deionized water. Cyclic voltammograms were acquired with the CH Instrument CHI630D potentiostat and recorded with CH Instruments software (version 13.04). All potentials are given with respect to the ferrocene-ferrocenium couple.

#### UV-vis spectroscopic studies

UV-vis spectra were recorded on a Hewlett Packard 8453 instrument. DFB was used as the solvent blank. In the glovebox, 0.29 mM solutions of  $\text{FcBAr}^{\text{F}}$ ,  $\text{CoCp}_2$ ,  $(\text{fc}^{\text{P},\text{B}})\text{NiBr}$ , and  $[(\text{fc}^{\text{P},\text{B}})\text{NiBr}][\text{BAr}^{\text{F}}]$  in DFB were

prepared in advance. 5 mL of the solution being measured was placed into a 1 cm quartz cuvette that could be sealed with a Schlenk cap, and UV-vis spectra were recorded. Before testing the next species, the cuvette was washed four times with DFB. For the *in situ* redox studies of  $(\text{fc}^{\text{P},\text{B}})\text{NiBr}$ , a 0.29 mM solution of  $(\text{fc}^{\text{P},\text{B}})\text{NiBr}$  in 5 mL DFB was added to the cuvette and a spectrum was recorded.  $\text{FcBAr}^{\text{F}}$  was weighed out in a glass vial and 1 mL of the 0.29 mM  $(\text{fc}^{\text{P},\text{B}})\text{NiBr}$  solution was used to dissolve the  $\text{FcBAr}^{\text{F}}$  before quickly transferring the resulting solution back into the cuvette. UV-vis spectra were recorded every 15 minutes for 2 h.  $\text{CoCp}_2$  was then weighed out in a separate glass vial and 1 mL of the 0.29 mM  $[(\text{fc}^{\text{P},\text{B}})\text{NiBr}][\text{BAr}^{\text{F}}]$  solution was used to dissolve the  $\text{CoCp}_2$  before quickly transferring the resulting solution back into the cuvette. UV-vis spectra were again recorded every 15 min for 2 h.

#### X-ray crystallography

X-ray quality crystals were obtained from a toluene solution layered with hexanes and placed in a -35 °C freezer in the glovebox. The X-ray data collections were carried out on a Bruker SMART 1000 single crystal X-ray diffractometer using  $\text{Cu K}\alpha$  radiation and a SMART APEX CCD detector. The data was reduced by SAINTPLUS and an empirical absorption correction was applied using the package SADABS. The structure was solved and refined using SHELXTL (Bruker 1998, SMART, SAINT, XPREP AND SHELXTL, Bruker AXS Inc., Madison, Wisconsin, USA). Tables with atomic coordinates and equivalent isotropic displacement parameters, with all the distances and angles and with anisotropic displacement parameters are listed in the cif.

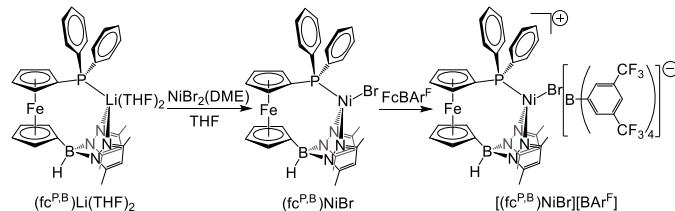
## Results and Discussion

#### Synthesis and characterization of the nickel bromide complex

$(\text{fc}^{\text{P},\text{B}})\text{NiBr}$  was synthesized by reacting  $(\text{fc}^{\text{P},\text{B}})\text{Li}\cdot(\text{THF})_2$  with  $\text{NiBr}_2(\text{DME})$  in THF at room temperature (Scheme 1).<sup>44</sup> Attempts to characterize  $(\text{fc}^{\text{P},\text{B}})\text{NiBr}$  via  $^1\text{H}$  NMR spectroscopy resulted in only broad, uninformative peaks as expected for a paramagnetic compound (Figure S10). The solid-state molecular structure of  $(\text{fc}^{\text{P},\text{B}})\text{NiBr}$  was determined by single-crystal X-ray diffraction (Figure 2). The coordination environment around the nickel center has a distorted tetrahedral geometry with a  $\tau$  value of 0.84.<sup>52</sup> The metal-ligand distances ( $\text{P}(1)\text{-Ni}(1)$ , 2.3235(7) Å;  $\text{Br}(1)\text{-Ni}(1)$ , 2.3488(4) Å;  $\text{N}(2)\text{-Ni}(4)$ , 1.9567(19) Å;  $\text{N}(1)\text{-Ni}(1)$ , 1.965(2) Å) match closely with those of the analogous  $(\text{fc}^{\text{P},\text{B}})\text{NiCl}$ .<sup>44</sup>

The redox behavior of  $(\text{fc}^{\text{P},\text{B}})\text{NiBr}$  was studied using cyclic voltammetry performed in a tetrabutylammonium hexafluorophosphate ( $[\text{TBA}][\text{PF}_6]$ ) solution in THF (Figure 2).  $(\text{fc}^{\text{P},\text{B}})\text{NiBr}$  displayed a quasi-reversible redox process at  $E_{1/2} = -0.09$  V vs  $\text{Fc}/\text{Fc}^+$  with an  $i_{\text{pc}}/i_{\text{pa}} = 1.65$ , and a second irreversible oxidation event at  $E_{1/2} = -1.62$  V vs  $\text{Fc}/\text{Fc}^+$ . This behavior differs significantly from  $(\text{fc}^{\text{P},\text{B}})\text{NiCl}$ , which displayed two reversible redox events at  $E_{1/2} = -0.03$  V and  $E_{1/2} = -1.58$  V vs  $\text{Fc}/\text{Fc}^+$  that were previously assigned to the ferrocene moiety and nickel, respectively.<sup>44</sup> Meanwhile, the *in situ* reactions with  $\text{FcBAr}^{\text{F}}$  ( $\text{Fc}$  = ferrocenium,  $\text{BAr}^{\text{F}}$  = tetrakis(3,5-bis(trifluoromethyl)phenyl)borate) as the oxidant<sup>51</sup> and  $\text{CoCp}_2$  (cobaltocene) as the reductant in a mixture of 1,2-difluorobenzene (DFB) and  $\text{C}_6\text{D}_6$  were monitored by  $^1\text{H}$  NMR spectroscopy (Figure S13). No obvious peaks were observed in the oxidized spectrum, and the return of the original broad peaks was not observed after reduction with  $\text{CoCp}_2$ , suggesting the original

compound could not be regenerated. A qualitative solution state magnetic susceptibility study further corroborated these results as the original difference in chemical shift of the internal standard could not be regenerated and the peak splitting became quite complex (Figure S14).<sup>53</sup> The color of the mixture changed during the oxidation and reduction processes, gradually from dark green to a dark-reddish brown, when the oxidation occurred over the course of two hours.



**Scheme 1.** Synthesis of  $(fc^{P,B})NiBr$  and  $[(fc^{P,B})NiBr][BAr^F]$  from  $(fc^{P,B})Li(THF)_2$ .

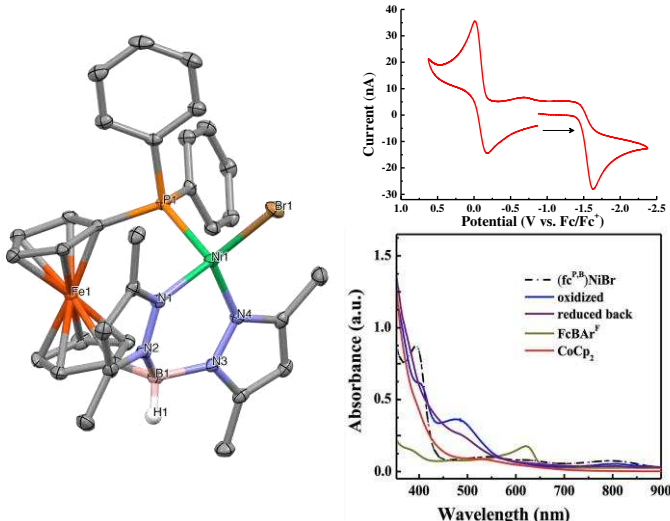


**Figure 2.** Left: Thermal ellipsoid (50% probability) representation of  $(fc^{P,B})NiBr$ ; hydrogen atoms (except for B-H) and co-crystallized toluene were omitted for clarity. Top right: Redox behavior of  $(fc^{P,B})NiBr$ ; cyclic voltammogram recorded with a glassy carbon electrode at 100 mV/s in THF, 0.10 M [TBA][PF<sub>6</sub>] containing 1.0 mM  $(fc^{P,B})NiBr$ .  $E_{1/2} = -0.09$  V, -1.62 V. Bottom right: UV-vis study of different  $(fc^{P,B})NiBr$  species (0.29 mM) in 1,2-difluorobenzene.

However, the return of the dark green color was not observed after the addition of  $CoCp_2$ . To help verify that the original compound is not restored upon reduction with  $CoCp_2$ , UV-vis data was collected (Figure 2). The absorbance at 392 nm in  $(fc^{P,B})NiBr$  slowly disappears and an absorbance at 488 nm appears as the compound is reacted with  $FcBAr^F$ . Upon reaction with  $CoCp_2$ , the absorbance at 392 nm is not regenerated, further indicating that the original compound cannot be regenerated.

Elemental analysis results of the reduced and oxidized states of  $(fc^{P,B})NiBr$  were in agreement with the calculated values. These data are consistent with an oxidized species being generated with  $FcBAr^F$ , and it was reasoned that the coordination of a substrate may enhance the stability of the catalytically active species. A similar situation was observed by us previously when investigating the effect of

the redox state of  $(thiolfan^*)Zr(NEt_2)_2$  ( $thiolfan^* = 1, 1'$ -bis(2,4-di-*tert*-butyl-6-thiophenoxy)ferrocene) on the hydroamination of primary and secondary aminoalkenes.<sup>54</sup>

### Homopolymerization reactions

The activity of  $(fc^{P,B})NiBr$  and  $[(fc^{P,B})NiBr][BAr^F]$  toward styrene, *p*-chlorostyrene (*p*-CS), methyl methacrylate (MMA), *n*-butyl methacrylate (*n*-BuMA), and acrylonitrile polymerization was investigated in order to ascertain the effect of redox states on reactivity in radical polymerization (Table 1). For styrene and MMA, only the oxidized compound was active, and no activity could be observed for the reduced state (Table 1, entries 1-2 and 5-6). MMA reached 91% conversion after 123 hours, while styrene reached full monomer conversion after only 0.1 hours (Figures S15, S17). Poly(styrene) (PS) and poly(methyl methacrylate) (PMMA), displayed a narrow unimodal distribution, with dispersities of 1.40 and 1.09, respectively (Figures S30, S32). Both *p*-CS and *n*-BuMA displayed preferential activity toward the reduced compound, achieving a 93% and 95% conversion after 44 hours, respectively (Table 2, entries 3-4 and 7-8). Poly(*p*-chlorostyrene) (PCS) and poly(*n*-butyl methacrylate) (*Pn*-BuMA) were well controlled and displayed a narrow unimodal distribution, with dispersities of 1.14 and 1.09, respectively (Figures S31, S33). Though *Pn*-BuMA obtained via the oxidized compound displayed a narrow unimodal distribution with a dispersity of 1.05, the conversion of the monomer was only 38% (Figure S19). Acrylonitrile was not active toward the oxidized nor the reduced compound. This is consistent with previous studies that used Cu-based catalysts,<sup>55,56</sup> and is likely due to the nitrile functional group being too strong of a nucleophile.<sup>45</sup> Relevant control studies (Table S1) performed in the absence of radical initiator show the likely formation of oligomers, and therefore a radical mechanism is favored.

### Copolymerization reactions

Encouraged by the orthogonal monomer selectivity described above, the synthesis of block copolymers was attempted via redox-switchable radical polymerization even though the oxidation reaction is not reversible. As shown in previous studies,<sup>15,54</sup> we hypothesize that in the presence of coordinating substrates, the stability of the oxidized species is enhanced, thus allowing for switchable reactivity.

To create an AB diblock, we started with the oxidized compound and polymerized styrene. This was followed by the addition of  $CoCp_2$  to alter the catalytic behavior of  $[(fc^{P,B})NiBr][BAr^F]$  and the addition of *p*-CS to start growing a *p*-CS block resulting in a PS-PCS copolymer with a relatively low *p*-CS conversion (Table 2, entry 2). The reverse diblock PCS-PS was also synthesized with greater success owing to not needing to switch the oxidized compound into a different catalytic state (Table 2, entry 4).

In both cases, the activity of the first block is similar to that observed from homopolymerization studies, but for the second block it was comparably slower, presumably due to decomposition or incomplete catalyst reduction as our catalyst state changes are not reversible under non-electrochemical conditions. While the SEC traces displayed narrow unimodal molecular weight distributions, diffusion order spectroscopy (DOSY) proved inconclusive for the PCS-PS copolymer since each block is of similar molecular weight (Figures S34, S39).

**Table 1.** Homopolymerization of various monomers by  $(fc^{P,B})NiBr$  and  $[(fc^{P,B})NiBr][BAr^F]$ .

Entry	Catalyst <sup>[a]</sup>	Monomer <sup>[b]</sup>	Time (h)	T (°C)	Conv. (%)	$Mn_{calc}$ (kg/mol) <sup>[c]</sup>	$Mn_{exp}$ (kg/mol) <sup>[d]</sup>	$D$ <sup>[d]</sup>
1	<b>red</b>	styrene	70	80	NR	-	-	-
2	<b>ox</b>	styrene	0.1	RT	>99	9.9	4.6	1.40
3	<b>red</b>	<i>p</i> -CS	44	80	93	11.4	12.6	1.14
4	<b>ox</b>	<i>p</i> -CS	44	RT	<20	N/D <sup>[e]</sup>	N/D <sup>[e]</sup>	N/D <sup>[e]</sup>
5	<b>red</b>	MMA	123	80	NR	-	-	-
6	<b>ox</b>	MMA	123	RT	91	9.8	10.1	1.09
7	<b>red</b>	<i>n</i> -BuMA	44	80	95	13.1	9.9	1.29
8	<b>ox</b>	<i>n</i> -BuMA	49	RT	38	4.9	3.0	1.05
9	<b>red</b>	acrylonitrile	27	80	NR	-	-	-
10	<b>ox</b>	acrylonitrile	27	RT	NR	-	-	-

Conditions: monomer (1.05 mmol), ethyl 2-bromo isobutyrate (0.0111 mmol),  $(fc^{P,B})NiBr$  (0.0111 mmol), 1,3,5-trimethoxybenzene (TMB) as an internal standard (0.1167 mmol),  $FcBAr^F$  as the oxidant (0.0111 mmol), and  $C_6D_6$  and *o*-difluorobenzene as the solvent (a total volume of 0.5 mL); [a] “red” and “ox” refer to the reduced and *in situ* generated oxidized compound. [b] *p*-CS = *p*-chlorostyrene, MMA = methyl methacrylate, *n*-BuMA = *n*-butyl methacrylate. [c] Determined by  $^1H$  NMR spectroscopy. [d] Determined by SEC. [e] Not determined.

**Table 2.** Redox controlled copolymerization studies by  $(fc^{P,B})NiBr$  and  $[(fc^{P,B})NiBr][BAr^F]$ .

Entry	Monomer	Monomer	Monomer	Catalyst <sup>[b]</sup>	Time (h)	T (°C)	Conv. (%)	$Mn_{calc}$	$Mn_{exp}$	$D$
	1 <sup>[a]</sup>	2	3					(kg/mol) <sup>[c]</sup>	(kg/mol) <sup>[d]</sup>	
1	styrene	-	-	<b>ox</b>	0.2	25	90	9.0	6.8	1.10
2	styrene	<i>p</i> -CS	-	<b>ox-red</b>	0.2-46	25-80	90-18	11.4	10.8	1.33
3	<i>p</i> -CS	-	-	<b>red</b>	21	80	77	9.4	10.1	1.18
4	<i>p</i> -CS	styrene	-	<b>red-ox</b>	21-44	80-25	77-72	16.6	15.5	1.17
5	<i>p</i> -CS	styrene	<i>p</i> -CS	<b>red-ox-red</b>	21-44-44	80-25-80	77-72-37	21.1	19.4	1.24

Conditions: monomer (1.05 mmol), ethyl 2-bromo isobutyrate (0.0111 mmol), 1,3,5-trimethoxybenzene (TMB) as an internal standard (0.1167 mmol),  $FcBAr^F$  as oxidant (0.0111 mmol),  $CoCp_2$  as reductant (0.0111 mmol), and  $C_6D_6$  and *o*-difluorobenzene as solvent. Reaction temperatures were based on homopolymer studies, unless otherwise mentioned. [a] *p*-CS = *p*-chlorostyrene. [b] “red” and “ox” refer to the reduced and *in situ* generated oxidized compound. [c] Determined by  $^1H$  NMR spectroscopy. [d] Determined by SEC.

However, using the Stejskal-Tanner equation,<sup>57</sup> it was clear that the two blocks in the copolymer have a similar diffusion coefficient, and that if the corresponding homopolymers were present, a faster diffusion coefficient would have been observed (Figure S8). Other diblock copolymers with a variety of monomer combinations were attempted (Table S2), but none of them formed copolymers despite literature precedence for block copolymers of *Pn*-BuMA-MMA<sup>38</sup> and *Pn*-BuMA-PS.<sup>58</sup>

Previous reports of PS-PCS diblock copolymers synthesized via radical polymerization required the use of a PS macroinitiator, and triblock copolymers were not attempted.<sup>59</sup> The only other example of PS and PCS ABA triblock copolymers was synthesized via anionic polymerization with sodium naphthalene.<sup>60</sup> Therefore, we set out to prepare ABA triblock copolymers of PCS and PS via radical polymerization and to ascertain if the catalytic activity of  $(fc^{P,B})NiBr$  was regained after sequential oxidation and reduction. While a PS-PCS-PS

copolymer could not be obtained (Table S2, entry 9), sequential addition of  $CoCp_2$  to the PCS-PS diblock reaction mixture followed by *p*-CS led to the formation of a third block, incorporating 37% of *p*-CS after 44 h at 80 °C (Table 2, entry 5). Despite the low conversion of the third block, the triblock copolymer exhibits a narrow unimodal distribution (Figure 3, Figure S40). DOSY results show only one diffusion coefficient (Figure S5), and the Stejskal-Tanner plot indicates that the blocks in PCS-PS-PCS triblock have a distinct diffusion coefficient from the blocks in PS-PCS diblock (Figure S9). Therefore, it is confirmed that *p*-CS was incorporated as a third block and a triblock copolymer was formed. Despite the fact that the reduced compound could not be recovered from independent reactions with chemical redox reagents, we hypothesize that coordinating substrates enhance the stability of the Ni complex, thus allowing a triblock copolymer to be formed. This is consistent with our other works where

additional switchable behavior is only observed in the presence of monomer.<sup>15,54</sup>

Interestingly, the block copolymers synthesized here are the first examples of copolymers made by exploiting the orthogonal reactivity of different oxidation states for radical polymerization systems. Switchable catalysis studies in ATRP tend to focus on electrochemically mediated reactions, where catalysts can only be switched on or off,<sup>61</sup> and the synthesis of block copolymers tends to start from macroinitiators,<sup>62-64</sup> unlike in the present system, which can synthesize block copolymers *de novo*. Expanding the realm of redox switchable catalysts from ring opening polymerizations to include the polymerization of polar vinyl monomers offers an opportunity to couple these systems in future work. The results presented herein are an important step toward achieving both increased complexity and increased temporal control in polymer synthesis.

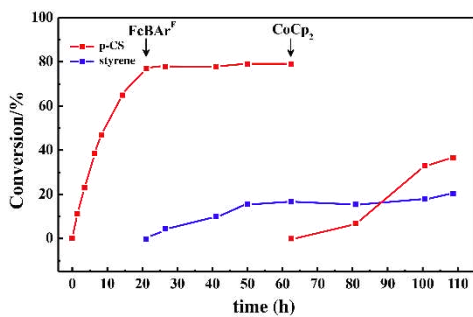


**Figure 3.** Plot of conversion (%) vs time for the sequential addition polymerization of *p*-CS and styrene with  $(fc^{P,B})NiBr$  using *in situ* oxidation and reduction with  $FcBar^F$  and  $CoCp_2$ , respectively.

## Conclusions

The application of a ferrocene-chelating heteroscorpionate ligand in nickel mediated radical polymerization was explored. In the presence of a radical initiator,  $(fc^{P,B})NiBr$  is active in *p*-CS and *n*-BuMA polymerization, while the oxidized species is active in styrene, *p*-MOS, and MMA polymerization. Even though the oxidized species could not be chemically reduced back to  $(fc^{P,B})NiBr$ , the catalytic nature of  $[(fc^{P,B})NiBr][Bar^F]$  could still be altered by the addition of a reductant, facilitating the preparation of PCS-PS, PS-PCS, and PCS-PS-PCS block copolymers via sequential monomer addition. These copolymers offer proof-of-concept that redox switchable catalysis can be expanded to radical polymerizations.

## Author Contributions

Shuangshuang Li: Conceptualization, investigation, formal analysis, visualization. Ashton R. Davis: Investigation, writing – original draft. Hootan Roshandel, Nima Adhami, Yi Shen, Nathalie H. Co: Investigation, writing – review and editing. Yuan Liu: Funding acquisition. Paula L. Diaconescu: Project administration, supervision, resources, funding acquisition, writing – review and editing.

## Conflicts of interest

There are no conflicts to declare.

## Acknowledgements

This work was supported by NSF CHE-1809116, Natural Science Foundation of China (Nos. 21872101) and the China Scholarship Council. Shuangshuang Li is grateful for the Qingdao Agricultural University Doctoral Startup Fund (655/1121017). Yi Shen is grateful for an INFEWS fellowship (NSF Grant DGE-1735325). EPR studies were supported by a shared instrumentation grant from the National Science Foundation, CHE-2117480. We thank Prof. Hannah Shafaat and Henry Teptarakulkarni for help with the acquisition of EPR data.

## Notes and references

- Blanco, V.; Leigh, D. A.; Marcos, V. Artificial switchable catalysts. *Chem. Soc. Rev.* **2015**, *44*, 5341-5370.
- Allgeier, A. M.; Mirkin, C. A. Ligand Design for Electrochemically Controlling Stoichiometric and Catalytic Reactivity of Transition Metals. *Angew. Chem. Int. Ed.* **1998**, *37*, 894-908.
- Chen, C. Redox-Controlled Polymerization and Copolymerization. *ACS Catal.* **2018**, *8*, 5506-5514.
- Wei, J.; Diaconescu, P. L. Redox-Switchable Ring-Opening Polymerization with Ferrocene Derivatives. *Acc. Chem. Res.* **2019**, *52*, 415-424.
- Deacy, A. C.; Gregory, G. L.; Sulley, G. S.; Chen, T. T. D.; Williams, C. K. Sequence Control from Mixtures: Switchable Polymerization Catalysis and Future Materials Applications. *J. Am. Chem. Soc.* **2021**, *143*, 10021-10040.
- Teator, A. J.; Lastovickova, D. N.; Bielawski, C. W. Switchable Polymerization Catalysts. *Chem. Rev.* **2016**, *116*, 1969-1992.
- Cunningham, L.; Benson, A.; Guiry, P. J. Recent developments in the synthesis and applications of chiral ferrocene ligands and organocatalysts in asymmetric catalysis. *Org. Biomol. Chem.* **2020**, *18*, 9329-9370.
- Hern, Z. C.; Quan, S. M.; Dai, R.; Lai, A.; Wang, Y.; Liu, C.; Diaconescu, P. L. ABC and ABAB Block Copolymers by Electrochemically Controlled Ring-Opening Polymerization. *J. Am. Chem. Soc.* **2021**, *143*, 19802-19808.
- Doerr, A. M.; Burroughs, J. M.; Gitter, S. R.; Yang, X.; Boydston, A. J.; Long, B. K. Advances in Polymerizations Modulated by External Stimuli. *ACS Catal.* **2020**, *10*, 14457-14515.
- Zhao, M.; Chen, C. Accessing Multiple Catalytically Active States in Redox-Controlled Olefin Polymerization. *ACS Catal.* **2017**, *7*, 7490-7494.
- Leibfarth, F. A.; Mattson, K. M.; Fors, B. P.; Collins, H. A.; Hawker, C. J. External Regulation of Controlled Polymerizations. *Angew. Chem. Int. Ed.* **2013**, *52*, 199-210.
- Broderick, E. M.; Guo, N.; Wu, T.; Vogel, C. S.; Xu, C.; Sutter, J.; Miller, J. T.; Meyer, K.; Cantat, T.; Diaconescu, P. L. Redox control of a polymerization catalyst by changing the oxidation state of the metal center. *Chem. Commun.* **2011**, *47*, 9897.
- Quan, S. M.; Wang, X.; Zhang, R.; Diaconescu, P. L. Redox Switchable Copolymerization of Cyclic Esters and Epoxides by a Zirconium Complex. *Macromolecules* **2016**, *49*, 6768-6778.
- Wei, J.; Riffel, M. N.; Diaconescu, P. L. Redox Control of Aluminum Ring-Opening Polymerization: A Combined Experimental and DFT Investigation. *Macromolecules* **2017**, *50*, 1847-1861.

(15) Abubekerov, M.; Vlček, V.; Wei, J.; Miehlich, M. E.; Quan, S. M.; Meyer, K.; Neuhauser, D.; Diaconescu, P. L. Exploring Oxidation State-Dependent Selectivity in Polymerization of Cyclic Esters and Carbonates with Zinc(II) Complexes. *iScience* **2018**, *7*, 120-131.

(16) Lai, A.; Hern, Z. C.; Diaconescu, P. L. Switchable Ring-Opening Polymerization by a Ferrocene Supported Aluminum Complex. *ChemCatChem* **2019**, *11*, 4210-4218.

(17) Xu, X.; Luo, G.; Hou, Z.; Diaconescu, P. L.; Luo, Y. Theoretical insight into the redox-switchable activity of group 4 metal complexes for the ring-opening polymerization of  $\epsilon$ -caprolactone. *Inorg. Chem. Front.* **2020**, *7*, 961-971.

(18) Biernesser, A. B.; Delle Chiaie, K. R.; Curley, J. B.; Byers, J. A. Block Copolymerization of Lactide and an Epoxide Facilitated by a Redox Switchable Iron-Based Catalyst. *Angew. Chem. Int. Ed.* **2016**, *55*, 5251-5254.

(19) Stößer, T.; Sulley, G. S.; Gregory, G. L.; Williams, C. K. Easy access to oxygenated block polymers via switchable catalysis. *Nat. Commun.* **2019**, *10*.

(20) Biernesser, A. B.; Li, B.; Byers, J. A. Redox-Controlled Polymerization of Lactide Catalyzed by Bis(imino)pyridine Iron Bis(alkoxide) Complexes. *J. Am. Chem. Soc.* **2013**, *135*, 16553-16560.

(21) Doerr, A. M.; Burroughs, J. M.; Legaux, N. M.; Long, B. K. Redox-switchable ring-opening polymerization by tridentate ONN-type titanium and zirconium catalysts. *Cat. Sci. Technol.* **2020**, *10*, 6501-6510.

(22) Delle Chiaie, K. R.; Yablon, L. M.; Biernesser, A. B.; Michalowski, G. R.; Sudyn, A. W.; Byers, J. A. Redox-triggered crosslinking of a degradable polymer. *Polym. Chem.* **2016**, *7*, 4675-4681.

(23) Wang, X.; Huo, Z.; Xie, X.; Shanaiah, N.; Tong, R. Recent Advances in Sequence-Controlled Ring-Opening Copolymerizations of Monomer Mixtures. *Chem. Asian J.* **2023**, *18*, e202201147.

(24) Feng, Q.; Yang, L.; Zhong, Y.; Guo, D.; Liu, G.; Xie, L.; Huang, W.; Tong, R. Stereoselective photoredox ring-opening polymerization of O-carboxyanhydrides. *Nat. Commun.* **2018**, *9*, 1559.

(25) Shawver, N. M.; Doerr, A. M.; Long, B. K. A perspective on redox-switchable ring-opening polymerization. *J. Polym. Sci.* **2023**, *61*, 361-371.

(26) Abubekerov, M.; Khan, S. I.; Diaconescu, P. L. Ferrocene-bis(phosphinimine) Nickel(II) and Palladium(II) Alkyl Complexes: Influence of the Fe-M (M = Ni and Pd) Interaction on Redox Activity and Olefin Coordination. *Organometallics* **2017**, *36*, 4394-4402.

(27) Shepard, S. M.; Diaconescu, P. L. Redox-Switchable Hydroelementation of a Cobalt Complex Supported by a Ferrocene-Based Ligand. *Organometallics* **2016**, *35*, 2446-2453.

(28) Shen, Y.; Shepard, S. M.; Reed, C. J.; Diaconescu, P. L. Zirconium complexes supported by a ferrocene-based ligand as redox switches for hydroamination reactions. *Chem. Commun.* **2019**, *55*, 5587-5590.

(29) Maity, R.; Birenheide, B. S.; Breher, F.; Sarkar, B. Cooperative Effects in Multimetallic Complexes Applied in Catalysis. *ChemCatChem* **2021**, *13*, 2337-2370.

(30) Lastovickova, D. N.; Teator, A. J.; Shao, H.; Liu, P.; Bielawski, C. W. A redox-switchable ring-closing metathesis catalyst. *Inorg. Chem. Front.* **2017**, *4*, 1525-1532.

(31) Lastovickova, D. N.; Shao, H.; Lu, G.; Liu, P.; Bielawski, C. W. A Ring-Opening Metathesis Polymerization Catalyst That Exhibits Redox-Switchable Monomer Selectivities. *Chem. Eur. J.* **2017**, *23*, 5994-6000.

(32) Varnado, C. D.; Jr; Rosen, E. L.; Collins, M. S.; Lynch, V. M.; Bielawski, C. W. Synthesis and study of olefin metathesis catalysts supported by redox-switchable diaminocarbene[3]ferrocenophanes. *Dalton Trans.* **2013**, *42*, 13251.

(33) Arumugam, K.; Varnado, C. D.; Sproules, S.; Lynch, V. M.; Bielawski, C. W. Redox-Switchable Ring-Closing Metathesis: Catalyst Design, Synthesis, and Study. *Chem. Eur. J.* **2013**, *19*, 10866-10875.

(34) Chen, M.; Yang, B.; Chen, C. Redox-Controlled Olefin (Co)Polymerization Catalyzed by Ferrocene-Bridged Phosphine-Sulfonate Palladium Complexes. *Angew. Chem. Int. Ed.* **2015**, *54*, 15520-15524.

(35) Dadashi-Silab, S.; Lorandi, F.; Fantin, M.; Matyjaszewski, K. Redox-switchable atom transfer radical polymerization. *Chem. Commun.* **2019**, *55*, 612-615.

(36) Dadashi-Silab, S.; Matyjaszewski, K. Iron Catalysts in Atom Transfer Radical Polymerization. *Molecules* **2020**, *25*, 1648.

(37) Gillies, M. B.; Matyjaszewski, K.; Norrby, P.-O.; Pintauer, T.; Poli, R.; Richard, P. A DFT Study of R-X Bond Dissociation Enthalpies of Relevance to the Initiation Process of Atom Transfer Radical Polymerization. *Macromolecules* **2003**, *36*, 8551-8559.

(38) Moineau, C.; Minet, M.; Teyssié, P.; Jérôme, R. Synthesis and Characterization of Poly(methyl methacrylate)-block-poly(n-butyl acrylate)-block-poly(methyl methacrylate) Copolymers by Two-Step Controlled Radical Polymerization (ATRP) Catalyzed by NiBr<sub>2</sub>(PPh<sub>3</sub>)<sub>2</sub>. *Macromolecules* **1999**, *32*, 8277-8282.

(39) O'Reilly, R. K.; Shaver, M. P.; Gibson, V. C. Nickel(II)  $\alpha$ -diimine catalysts for the atom transfer radical polymerization of styrene. *Inorg. Chim. Acta* **2006**, *359*, 4417-4420.

(40) Braunecker, W. A.; Matyjaszewski, K. Controlled/living radical polymerization: Features, developments, and perspectives. *Prog. Polym. Sci.* **2007**, *32*, 93-146.

(41) Matyjaszewski, K. Atom Transfer Radical Polymerization (ATRP): Current Status and Future Perspectives. *Macromolecules* **2012**, *45*, 4015-4039.

(42) Tang, W.; Kwak, Y.; Braunecker, W.; Tsarevsky, N. V.; Coote, M. L.; Matyjaszewski, K. Understanding Atom Transfer Radical Polymerization: Effect of Ligand and Initiator Structures on the Equilibrium Constants. *J. Am. Chem. Soc.* **2008**, *130*, 10702-10713.

(43) Sunsin, A.; Wisutsri, N.; Suriyarak, S.; Teanchai, R.; Jindabot, S.; Chaicharoenwimolkul, L.; Somsook, E. Effect of ferrocene moieties on the copper-based atom transfer radical polymerization of methyl methacrylate. *J. Appl. Polym. Sci.* **2009**, *113*, 3766-3773.

(44) Abubekerov, M.; Diaconescu, P. L. Synthesis and Characterization of Ferrocene-Chelating Heteroscorpionate Complexes of Nickel(II) and Zinc(II). *Inorg. Chem.* **2015**, *54*, 1778-1784.

(45) Abubekerov, M.; Shepard, S. M.; Diaconescu, P. L. Switchable Polymerization of Norbornene Derivatives by a Ferrocene-Palladium(II) Heteroscorpionate Complex. *Eur. J. Inorg. Chem.* **2016**, *2016*, 2634-2640.

(46) Uegaki, H.; Kotani, Y.; Kamigaito, M.; Sawamoto, M. Nickel-Mediated Living Radical Polymerization of Methyl Methacrylate1. *Macromolecules* **1997**, *30*, 2249-2253.

(47) Duquesne, E.; Degée, P.; Habimana, J.; Dubois, P. Supported nickel bromide catalyst for Atom Transfer Radical Polymerization (ATRP) of methyl methacrylate. *Chem. Commun.* **2004**, *640*-641.

(48) Granel, C.; Dubois, P.; Jérôme, R.; Teyssié, P. Controlled Radical Polymerization of Methacrylic Monomers in the Presence of a Bis(ortho-chelated) Arylnickel(II) Complex and Different Activated Alkyl Halides. *Macromolecules* **1996**, *29*, 8576-8582.

(49) Uegaki, H.; Kotani, Y.; Kamigaito, M.; Sawamoto, M. NiBr<sub>2</sub>(Pn-Bu<sub>3</sub>)<sub>2</sub> Mediated Living Radical Polymerization of

Methacrylates and Acrylates and Their Block or Random Copolymerizations. *Macromolecules* **1998**, *31*, 6756-6761.

(50) Amy B. Pangborn, M. A. G., Robert H. Grubbs, Robert K. Rosen, and Francis J. Timmers. Safe and Convenient Procedure for Solvent Purification. *Organometallics* **1996**, *15*, 1518-1520.

(51) Chávez, I.; Alvarez-Carena, A.; Molins, E.; Roig, A.; Maniukiewicz, W.; Arancibia, A.; Arancibia, V.; Brand, H.; Manuel Manríquez, J. Selective oxidants for organometallic compounds containing a stabilising anion of highly reactive cations:  $(3,5(\text{CF}_3)_2\text{C}_6\text{H}_3)_4\text{B}^-$  and  $(3,5(\text{CF}_3)_2\text{C}_6\text{H}_3)_4\text{B}^-)\text{Cp}^*_2\text{Fe}^+$ . *J. Organomet. Chem.* **2000**, *601*, 126-132.

(52) Yang, L.; Powell, D. R.; Houser, R. P. Structural variation in copper(I) complexes with pyridylmethylamide ligands: structural analysis with a new four-coordinate geometry index,  $\tau_4$ . *Dalton Trans.* **2007**, 955-964.

(53) Evans, D. F. The determination of the paramagnetic susceptibility of substances in solution by nuclear magnetic resonance. *J. Chem. Soc.* **1959**, 2003-2005.

(54) Shen, Y.; Shepard, S. M.; Reed, C. J.; Diaconescu, P. L. Zirconium Complexes Supported by a Ferrocene-Based Ligand as Redox Switches for Hydroamination Reactions. *Chem. Commun.* **2019**, *55*, 5587-5590.

(55) Matyjaszewski, K.; Jo, S. M.; Paik, H.-j.; Shipp, D. A. An Investigation into the CuX/2,2'-Bipyridine (X = Br or Cl) Mediated Atom Transfer Radical Polymerization of Acrylonitrile. *Macromolecules* **1999**, *32*, 6431-6438.

(56) Barboiu, B.; Percec, V. Metal Catalyzed Living Radical Polymerization of Acrylonitrile Initiated with Sulfonyl Chlorides. *Macromolecules* **2001**, *34*, 8626-8636.

(57) Stejskal, E. O.; Tanner, J. E. Spin Diffusion Measurements: Spin Echoes in the Presence of a Time-Dependent Field Gradient. *J. Chem. Phys.* **1965**, *42*, 288-292.

(58) Jianying, H.; Jiayan, C.; Jiaming, Z.; Yihong, C.; Lizong, D.; Yousi, Z. Some monomer reactivity ratios of styrene and (meth)acrylates in the presence of TEMPO. *J. Appl. Polym. Sci.* **2006**, *100*, 3531-3535.

(59) Butz, S.; Hillermann, J.; Schmidt-Naake, G.; Kressler, J.; Thomann, R.; Heck, B.; Stühn, B. Synthesis and microphase separation of diblock copolymers of styrene and p-chlorostyrene prepared by using N-oxyl capped macroinitiators. *Acta Polym.* **1998**, *49*, 693-699.

(60) Shima, M.; Yamaguchi, N.; Sato, M.; Ogawa, E. Dipole moments of (styrene-p-chlorostyrene) triblock copolymers in solutions. *Eur. Polym. J.* **1983**, *19*, 601-604.

(61) De Bon, F.; Fantin, M.; Isse, A. A.; Gennaro, A. Electrochemically mediated ATRP in ionic liquids: controlled polymerization of methyl acrylate in [BmIm][OTf]. *Polym. Chem.* **2018**, *9*, 646-655.

(62) Chmielarz, P.; Krys, P.; Park, S.; Matyjaszewski, K. PEO-b-PNIPAM copolymers via SARA ATRP and eATRP in aqueous media. *Polymer* **2015**, *71*, 143-147.

(63) Chmielarz, P.; Park, S.; Simakova, A.; Matyjaszewski, K. Electrochemically mediated ATRP of acrylamides in water. *Polymer* **2015**, *60*, 302-307.

(64) Park, S.; Cho, H. Y.; Wegner, K. B.; Burdynska, J.; Magenau, A. J. D.; Paik, H.-J.; Jurga, S.; Matyjaszewski, K. Star Synthesis Using Macroinitiators via Electrochemically Mediated Atom Transfer Radical Polymerization. *Macromolecules* **2013**, *46*, 5856-5860.